

Load Testing for I-Girder type Bridge to Identify Serviceability, Load-carrying Capacity and Dynamic Response

Mustafa Khalid Rzaij Al-Nasar and Faiq Mohammed Sarhan Al-Zwainy

University of Al-Nahrain

Abstract - Most countries are facing several challenges and difficulties when it comes to managing deteriorating structures and evaluating the structure's remaining service life. One of the most essential things gaining speed the deterioration process is the shortage of regulations and rules controlling traffic. A Structure Health Monitoring system aims to accurately and effectively monitor a structure's behaviour identify damage or deterioration. It was chosen one of the bridges in the Republic of Iraq that were subjected to overloading and unusual traffic for this study to determine the bridge's overall performance and response to these loads. for the first time in Iraq, it was developed a structural health monitoring system for the Al-Shuhadah Bridge. Many sensors are connected to the data acquisition device, including LVDT, strain gauges and accelerometers distributed across the spans. The bridge was then subjected to a load test. The deflections, distribution factors, neutral axis position, curvatures modal, load rating, and bridge dynamic behaviour were extracted, and it was discovered that all of these indices values are reported to be lower than AASHTO specifications, with no unnatural conditions observed.

Index Terms – Structural Health Monitoring, Bridge, Concrete Bridge, Steel Bridge, Load Testing, Distribution Factor, Load Rating, Dynamic Response.

Introduction

Many of the challenges and difficulties faced by most developing as well as developed countries equivalent concerning their deteriorating structures are recognized. It is important to invest in the maintenance of existing structures, which have been identified as dilapidated and in need of restoration, as much as investment in the building of new structures constantly. This is particularly evident in developing countries like Iraq. Iraq and its decision-makers lack a culture of maintenance, which leads to high costs in the issue of failure or significant deterioration, which leads to total replacement. In this context, monitoring and evaluation techniques can significantly improve future decision-making.

Bridge load testing is frequently used to identify problems that are just not easily rectified by visual inspection. To resolve difficulties with a bridge or a group of bridges, visual inspection, load testing, structural health monitoring (SHM), non-destructive testing (NDT), and finite element (FE)-based structural modelling are mostly used. AASHTO-MBE[1, 25], for example, proposes load testing for determining the structural condition. The load test aims may differ from case to case, and such a test may be required on a specific bridge or a group of comparable bridges in order to make recommendations about bridge closure, load posting, replacement, and retrofit.

Various research papers in a similar field are studied and referred for this study. The researchers [2-5] explained and presented an overview of the bridge's behaviour under typical loads and the validity of these bridges to carry such loads in these investigations, which evaluated the health situation of I-girder bridges. A load test was performed [3] on one of the bridges with steel girders to extract the bridge's characteristics, and it was discovered that the bridge is appropriate for long-term operation. One of the papers [5] looked at an old bridge to see whether it could be used to extract fatigue and determine its remaining service life.

The researchers, on the other hand, provided novel techniques and approaches for using bridge health monitoring. Many articles [6-8] utilise deep learning technology to train a computer to assess the location and severity of damage by inputting experimental data. Deep learning technology combines artificial intelligence and machine learning to determine the location and severity of damage by entering experimental data. The Fuzzy Krill Herd [8], Artificial Neural Networks (ANN) [6], and Convolutional Neural Networks (CNN) [7] were all discussed. The machine's technology demonstrated the relevance and capability of detecting damage, and it may be utilised more broadly in the future. In previous papers, the development and study of bridge Weigh-in-Motion (BWIN) technology were essential [9-12]; this technology reveals the number of axles and wheel weights that affect the bridge. The researchers employed FAD sensors [9], acoustic emissions [11], and optical fibre sensors [12]. In the field of SHM, these devices and technologies have shown to be quite beneficial. Cameras were also utilized to collect and identify the bridge response in positions where traditional sensors are difficult to install [13, 14]. The researchers concluded that using this approach could produce more accurate experimental results than using conventional sensors [13]. The strain gauge was only utilised in one study [15] to obtain bridge response and displacement data. This enables the strain gauge to extract displacement in locations where an LVDT would be difficult to attach or install on a bridge.

Characterization of Case Study

Al-Shuhadah Bridge was chosen as the case study of this work representing the typical bridge's superstructure used in Iraq. The bridge selected for study is located in Al-Muthanna province in the south of Iraq and crosses the Euphrates River, as shown in Figure 1.

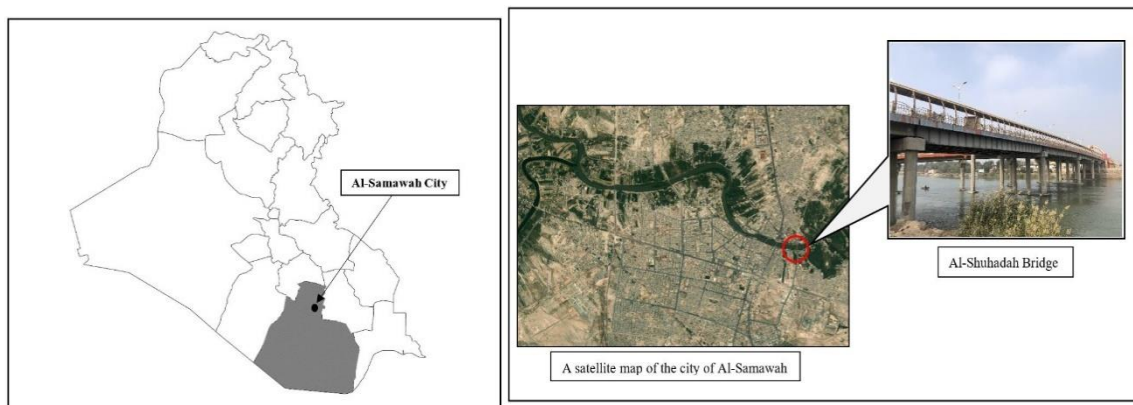


Figure 1 Location of Al-Shuhadah

The length of Al-Shuhadah Bridge is 356 metres and the width is 15.5 metres. The carriageway of the bridge contains four-lane; two-lane forward and two-lane backward; The Bridge is made up of seven simply supported spans as shown in Figure 3. Initially, the first two spans are 20 metres long, and the third spans out to 30 metres. The following two spans are 36 metres in length. In all, the last two spans are 23 metres across each other. The longitudinal girders are continuous as simply supported over the seven spans of the 188 m crossing. These girders are of two types, one is as pre-tension concrete and the other is a built-up steel girder. Pre-tensioned girders are used in spans 1, 2, 6, and 7, while built-up steel girders are used in spans 3, 4, and 5. Figure 3 show the superstructure for the bridge.

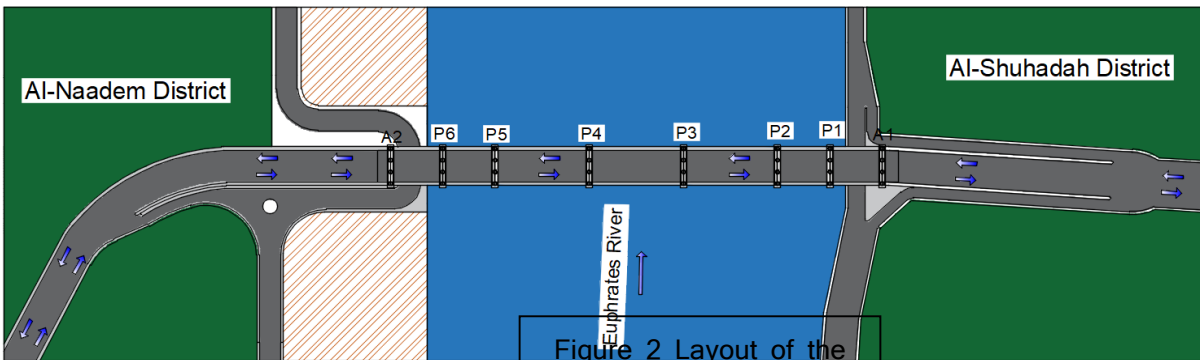
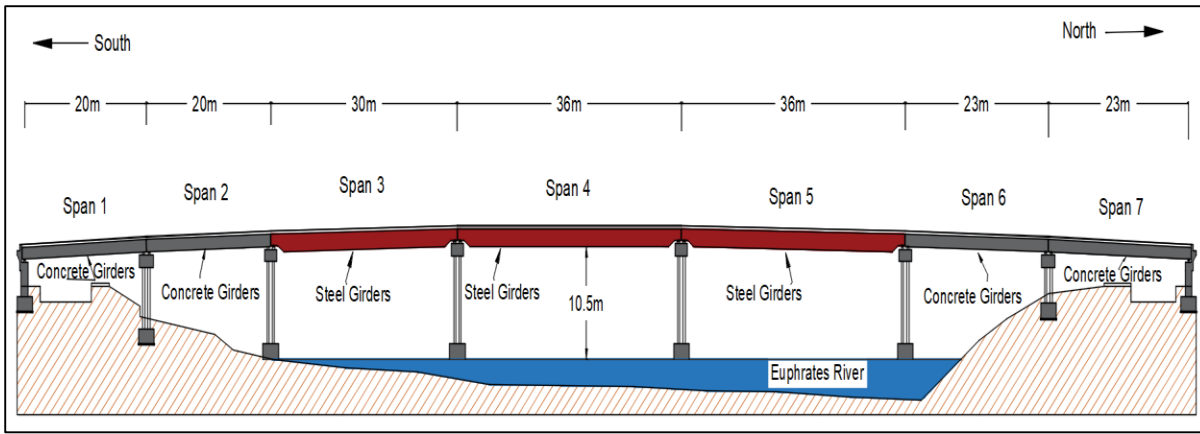
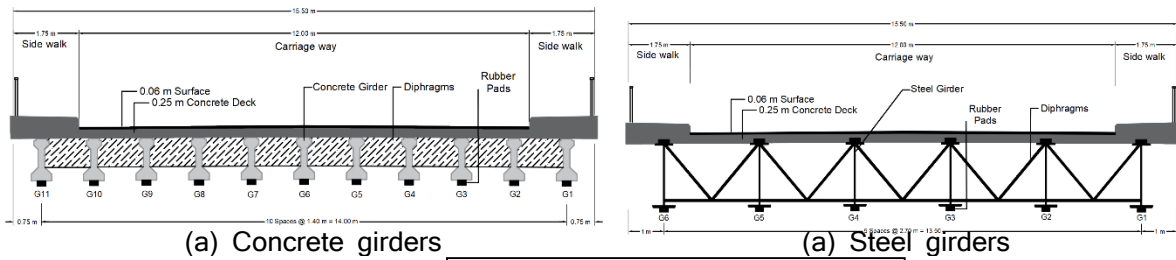


Figure 2 Layout of the



(a) Concrete girders

(a) Steel girders

Figure 3 Superstructure of the

Load Rating

This structure was designed to withstand military live loads of tracked vehicles Class 100 from (Iraqi standard specifications for road bridges). Figure 4 illustrates the loading pattern, for this loading class, which consists of a bogie 907 KN truck.

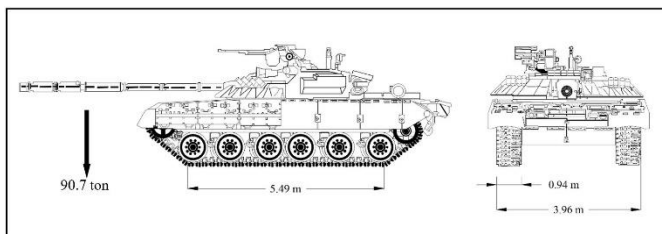


Figure 4 Military Live Loads Vehicles Class 100 From

Instrumentation Plan

The data acquisition system in our field testing was developed through the use of Arduino boards in combination with one of the most famous engineering software, LabVIEW [20]. In addition to LabVIEW software, Arduino boards have been employed in the development of this system. As shown in Figure 5, finally, the data acquisition device was set up with 14 data collection channels and a maximum collection rate of 200 samples/second/channel.

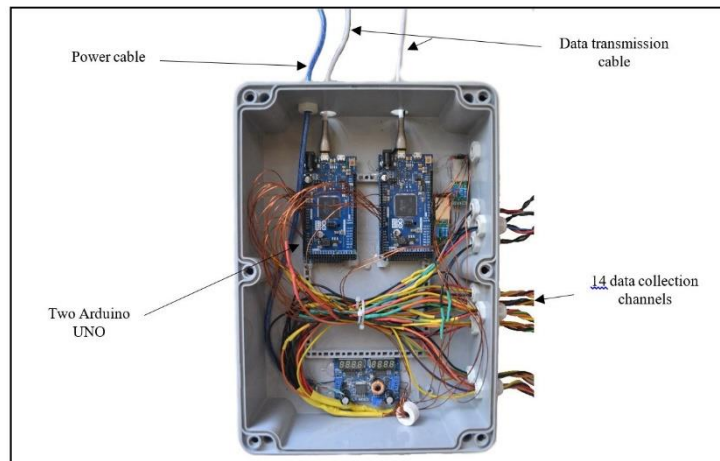
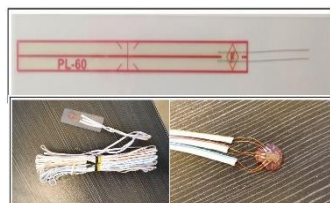


Figure 5 The data acquisition

Two strain gauges, two displacement sensors (LVDT) and six accelerometers were utilised and installed on the bridge in our case study. The main objective of this instrumentation was to record the structural system's overall behaviour. The type of sensors and its specification was displayed in Figure 6.



(a) LVDT Sensor



(b) Strain gauges PL-60-



(c) ADXL335 3-

Figure 6 Type of Used

The second span was picked from the south side of the bridge since all of the spans with concrete girders are identical. In terms of steel spans, the middle span (Span 4) was chosen since it is the longest and sits in the middle of the bridge structure. The forward traffic lanes, which begin on the bridge's southern side, consist of straight approaches, allowing the test vehicle's speed to be controlled, in contrast to what we notice on the opposite side (the northern side) which is a curved road. The implementation of sensors on the girders at the bottom of the forward lanes, that is, east of the bridge structure, was motivated by these reasons. For several days, ADT (average daily traffic) was monitored in the above-mentioned forward lanes. This provides us with an idea of which lanes have the most vehicles passing through. We note that roughly 90% of all vehicles travel in the second lane, also known as the "fast lane," while 10% go in the first lane, often known as the "slow lane". This leads us to monitor the second traffic lane, as

we are the ones who installed the sensors below the girders that sustain it. The fifth girder of span 2 and the third girder of span 4 was chosen as the target girder for putting the sensors because they are in the centre of the traffic lane, Figure 7.

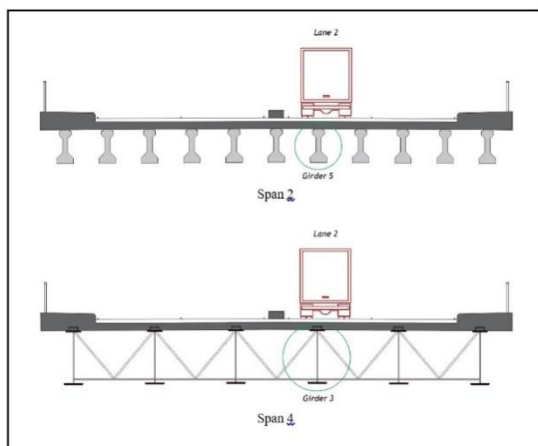


Figure 7 Selected Girders Locations for

In the investigation that is conducted in previous studies, S. Faraz et al. [10] declared that a girder in the middle of the lane receives the largest loads, bending moment, and stresses. Finally, the positions of all the sensors deployed on the Al-Shuhadah Bridge in longitudinal and top views were illustrated in Figure 8.

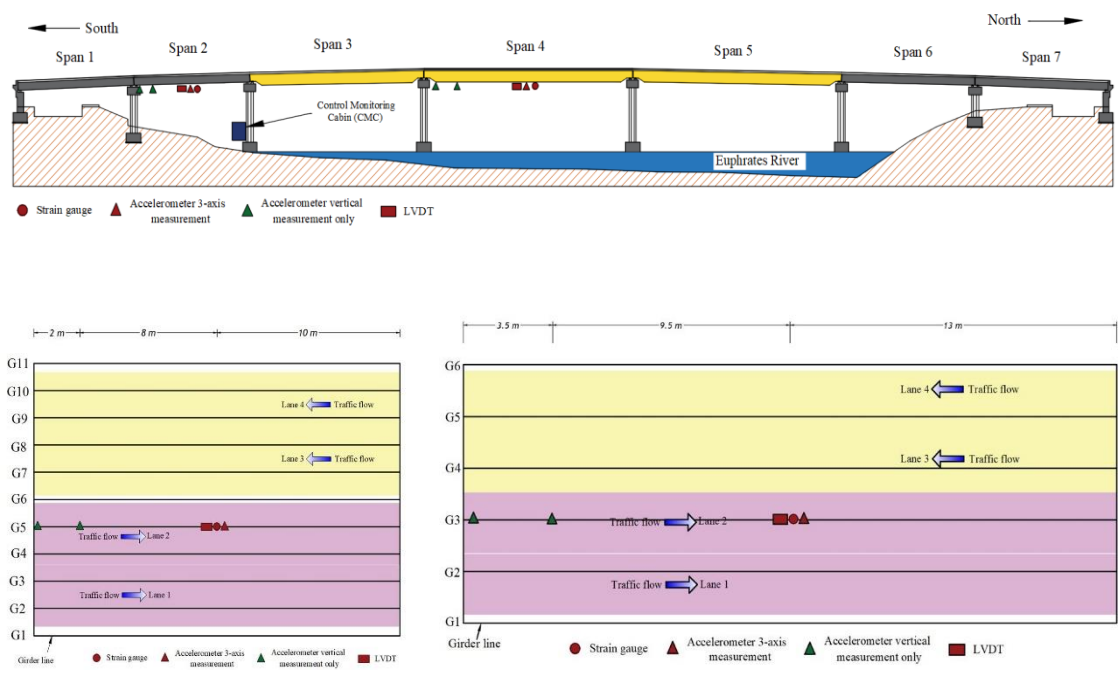


Figure 8 Locations of sensors; plan and

Load Testing

There were static, pseudo-static, and dynamic tests were performed on 2021\05\21 between 04:00 to 06.00 AM to evaluate the bridge's performance due to daily traffic and test truck. The Mercedes-Benz SK 3544 8x4 dump truck used in this study is shown in Figure 9 and the scenarios of static and dynamic cases were designed to implement the different tests. The test load level must be representative of serviceability situations. It is preferable to aiming for a load lev-

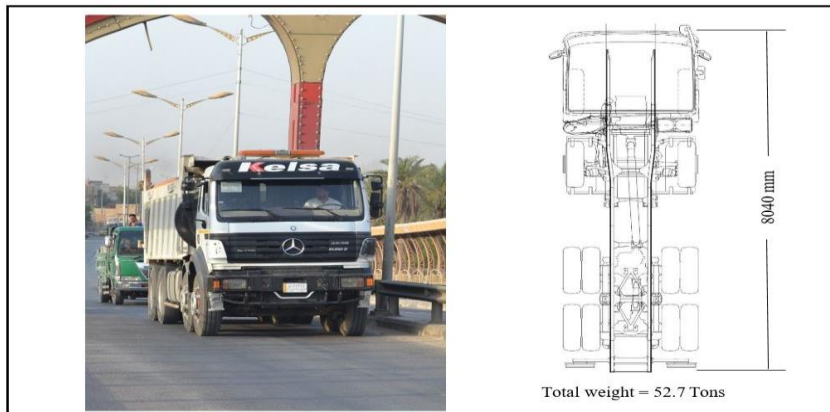


Figure 9 The Test

el that corresponds to a 5-year return time. In practice, this involves increasing the test load to around 60% of the characteristic live load specified in the design code. Never exceed 70% of the design load or 100% of the un-factored traffic load, according to regulatory requirements [3, 21, 22]. The weight of the truck is 18.4 Tons, and the total weight of the truck with load is 52.7 Tons; the trucks loads represented about 60% of the design loads of the bridge. During a calibration test, the time histories of each designed vehicle were recorded as it crossed the bridge in each travel lane while ordinary traffic was temporarily stopped in all directions.

The most common type of load test is static testing [21]. Vehicle loads with established axle weights represent the test load, which were placed at sections A-A, B-B, C-C and D-D in both spans (span 2 and span 4), Figure 10, to obtain the maximum load effect

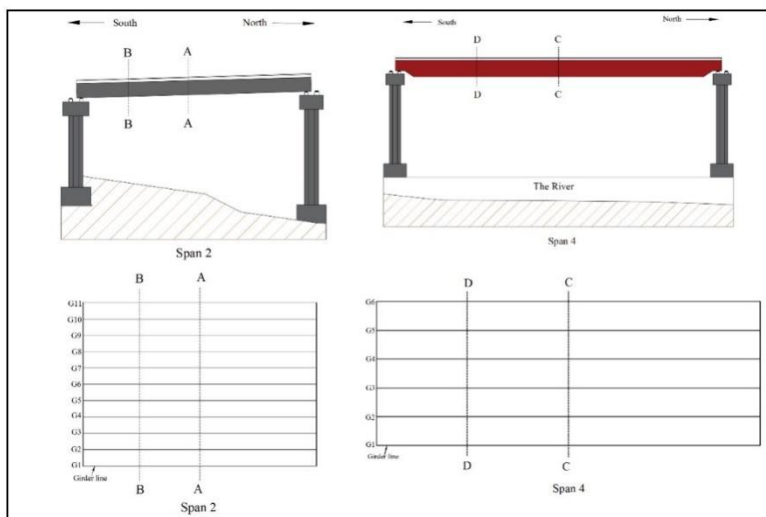


Figure 10 Test sections on the bridge (longitudinal)

Thus, four static and two pseudo-static tests are implemented to evaluate the bridge. Table 1 summarized the static and pseudo-static cases.

In the dynamic loading cases, the bridge was tested in one direction, Al-Shuhadah district to Al-Naadem district, over the second lane with the truck moving at different speeds, Figure 11. Table 2 presents the truck speeds and directions

Table 2 Dynamic loads scenarios

Load case	Direction	Lane	Speed
DC1	Forward	2	10 km/h
DC2	Forward	2	20 km/h
DC3	Forward	2	30 km/h
DC4	Forward	2	40 km/h
DC5	Forward	2	60 km/h
DC6	Forward	2	10 km/h
DC7	Forward	2	20 km/h
DC8	Forward	2	30 km/h
DC9	Forward	2	40 km/h
DC10	Forward	2	60 km/h

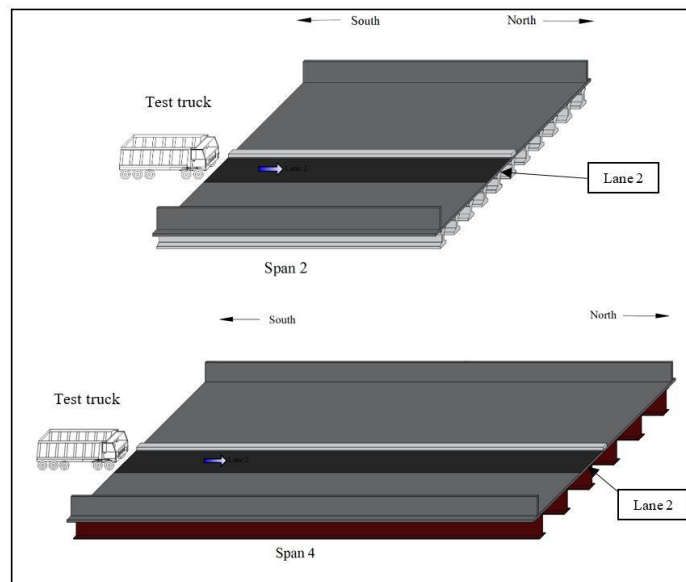


Figure 11 Dynamic test

Building and Updating a Finite Element Model

The bridge's FE model was created utilising beam elements and shell elements for the reinforced concrete pre-stress or built-up steel girders and deck, as illustrated in Figure 12. In addition, tendon elements were included in the studies to account for the pre-stress effect, and shell elements were used to simulate steel girders in steel. According to the bridge's calculation report and project drawings, all considerations for the FEM were achieved. The structural analysis software CSI-Bridge V.22 [18, 19] was used to achieve this goal. The bridge was then updated based on the experimental field test's modal characteristics and displacement results [17, 28]. The distribution factor and load rating of the updated FEM are also taken into account for the purpose of the comparison of experimental and AASHTO calculation.

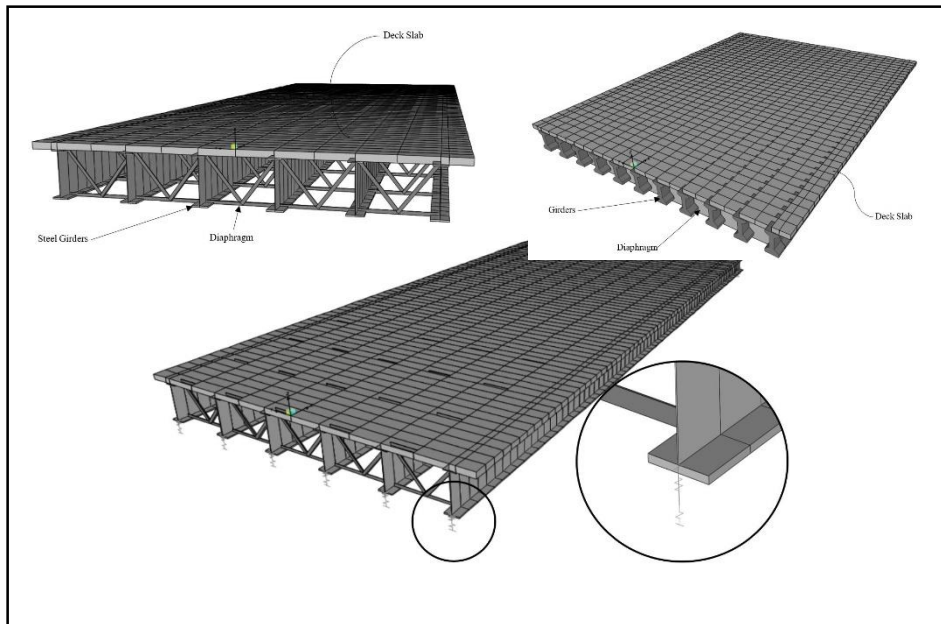


Figure 12 FE Model for Concrete and

Static Behavior Evaluation

The load test results can be utilised to gain a basic idea of how each of the bridge's girders responds to vehicle loads. When more complicated behaviours develop, simple observations in this respect enable relevant comparisons to be formed between the performance of the cases. In this procedure, comparisons between measured data and predicted responses obtained from FEM and fundamental strength of materials principles are also beneficial. To assess the load test findings, an attempt was made to separate the behaviour of the girders from the contributions of other bridge structural parts. In this regard, the present study focused on the girders' reaction, which was thought to be the most affected by the moving vehicles [24]. As a result, the following analysis of live load data concentrates on recorded displacements and strains. In addition, static evaluation is used to assess a structure's linear behavior [3]. The test may also be used to verify and update the load capacity of bridges.

The primary goal of the evaluation Al-Shuhadah Bridge is ultimately to compare the performance of the static and dynamic cases. The following sections present an analysis of several fundamental behaviours that have been computed. Each behaviour provides useful information on the baseline state of each factor to be computed, as well as how they behaved in comparison to one another.

Finally, it is important to mention that the steel grade and concrete capacity and AASHTO specifications code are used to evaluate the safety of the bridge. ST52-3 steel-grade girders, with 345 MPa yield strength and 270 MPa allowable tensile stresses and 200 GPa modulus of elasticity (E) is used.

Deflection Limits Check

The deflection limit check determines if the maximum mid-span displacement exceeds the value determined by $(L/800)$. This limit is frequently used to assess the bridge's serviceability [1, 23]. Here (L) is the length of the span, which is 20 m (20,000 mm) for span no.2 and is 36 m (36,000 mm) for span no.4. Here the limits of deflection is $(L_2 / 800 = 20000/800 = 25 \text{ mm})$ and $(L_4 / 800 = 36000/800 = 45 \text{ mm})$. As demonstrated in Table 3, the maximum displacement of mid-span collected from experimental test and FEM of girder 5 in span 2 and girder 3 in span 4 in static and semi-static cases are shown, which is considerably less than the serviceability deflection limit. This finding can be slightly predictable due to the number of girders and the length of the span. Finally, the bridge satisfies the requirements of AASHTO (2017) for serviceability

Table 3 Different experimental and FEM measurements with AASHTO specification

Case		Experimental (mm)	FEM (mm)	AASHTO (mm)
Span 2	SC1	1.522	1.676	25
	SC2	0.78	0.878	25
	PC1	1.934	2.498	25
Span 4	SC3	4.621	4.37	45
	SC4	1.28	1.46	45
	PC2	4.4	5.026	45
Case		Experimental (mm)	FEM (mm)	AASHTO (mm)
Span 2	SC1	1.522	1.676	25
	SC2	0.78	0.878	25
	PC1	1.934	2.498	25
Span 4	SC3	4.621	4.37	45
	SC4	1.28	1.46	45
	PC2	4.4	5.026	45
Case		Experimental (mm)	FEM (mm)	AASHTO (mm)
Span 2	SC1	1.522	1.676	25
	SC2	0.78	0.878	25
	PC1	1.934	2.498	25
Span 4	SC3	4.621	4.37	45
	SC4	1.28	1.46	45
	PC2	4.4	5.026	45

Distribution Factors (DF)

We can calculate load distribution factors of the bridge based on the responses across the bridge, which is important for bridge response and load rating. The DF may be computed using Equation (1) below and the displacement and strain results of each girder:

$$DF_i = \frac{\delta_i, \epsilon_i}{\sum_{j=1}^n \delta_j, \epsilon_j}$$

i, j = girder number,

δ, ϵ = the displacement or strain of the girder

On the other hand, AASHTO specifies formulas for estimating DF based on the geometry of the bridge's superstructure and single or multiple loading scenarios. The specific formulas for calculating the DF were obtained based on the geometry of the superstructure of the bridge utilised in our study, which is a composite superstructure with built-up steel girders and precast concrete girders (Table 4.6.2.2.2b-1 in AASHTO 2017) [1]. DF may be calculated using the previous equations within AASHTO's tables and

the bridge parameters for both the concrete (No. 2) and steel (No. 4) spans. According to the specifications of the AASHTO code, we chose the highest distribution factors, regardless of the loaded cases, as noted previously. The load distribution factors DF for the span 2 are (0.43) for the interior girders and (0.55) for the exterior girders. For span 4, the DF for the interior and exterior girders is (0.63). Table 4 shown DF that calculated by AASHTO formulas.

Span type	DF from AASHTO	
	Interior girders	Exterior girders
Concrete span (span no.2)	0.43	0.55
Steel span (span no.4)	0.63	0.63

The load distribution factor was practically calculated using the data of the strains and displacements obtained for all of the girders and Equation 1. Figure 13 compares the load distribution factor computed using AASHTO's formulae to that determined for SC1 and SC3 cases.

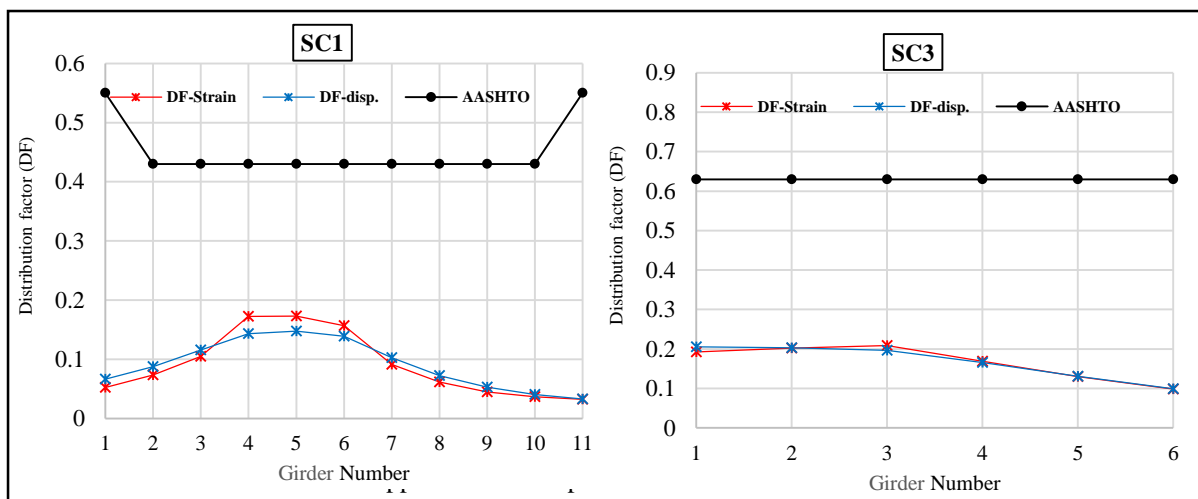


Figure 13 DF for SC1 and

the previous figures. Furthermore, the distribution factor DF had the highest values under the truckload. In the load case (DC1), the highest DF of span No.2 determined from displacements was (0.152), while the highest computed from strain was (0.19) for the same load case. The highest DF obtained from displacements in span No.4 was (0.21) in the load case (DC6), meanwhile the highest determined from strain measurements was (0.23) in the load case (SC4). The maximum DF value (0.23) indicates that the load distribution over the bridge is good.

The values of DFs estimated using the AASHTO formula give more conservative values, especially in the girders further away from the loaded lane, as illustrated in the previous figures. The AASHTO requirements, which involve taking the highest value obtained by the equations described at the beginning of this section, which is frequently the value extracted from the equations for multiple traffic lanes, resulted in the high DFs values computed through the AASHTO formulas. In our study, the cases were for one traffic lane loading. As a result, we created multiple lane loading scenarios that are more realistic than single-lane loading using the calibrated FEM. Figure 14 displays four new loading cases, each of which consists of two adjacent traffic lanes and two opposing traffic lanes. Finally, the DFs for multi-lane loading were discovered, and it was realised that they are still less than the values computed by AASHTO

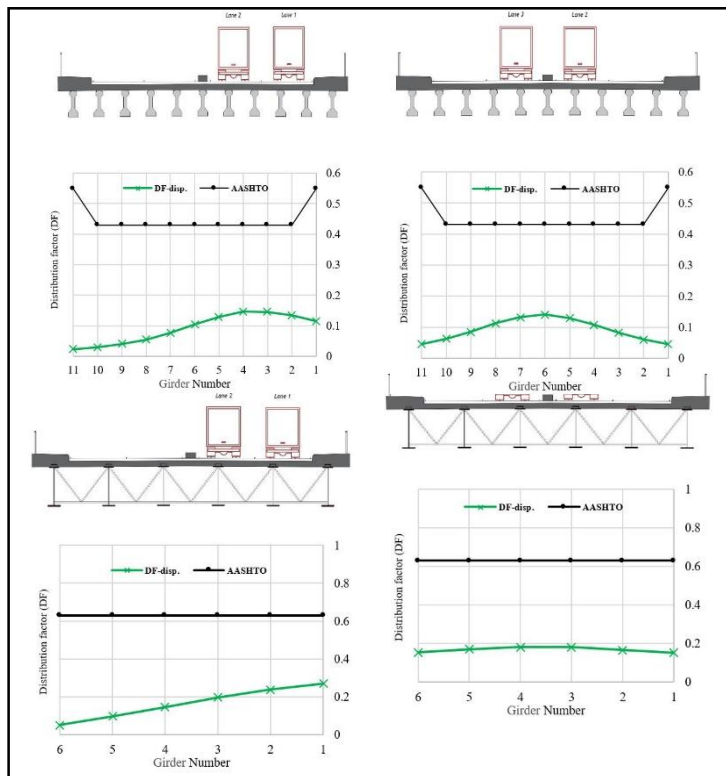


Figure 14DF for multi-loaded lanes

Load Rating (RF)

The bridge load rating is a defined method for determining a bridge's safe load-carrying capacity. In bridge management systems, operators utilize load ratings to optimize maintenance and repair funding. The structural condition, material characteristics, loads, and site traffic situations all play a role in determining a bridge load rating. Each component affects the bridge's condition and, as a result, the load rating. The primary objective of bridge load rating is to measure the condition of specific bridge components to ensure public safety.

The Manual for Bridge Evaluation (MBE) [25] by AASHTO provides recommendations on bridge load rating. The technique of testing live load response to specified AASHTO loads is known as bridge load rating. The MBE establishes a standard evaluation technique as well as a framework for determining the safe load capacity. Using the values of the DFs from the previous section and the test truck load, a basic frequently used method for calculating the load rating factor may be determined using AASHTO formulas. For Strength Limit I, the rating factors (RF) are computed using DF and the test truck. With Equation 2, AASHTO (2017) provides a general formulation for load rating:

$$RF = \frac{C - \gamma_{DC}DC - \gamma_{DW}DW}{\gamma_{LL}(LL + IM)} \tag{1}$$

In which, C denotes the current load-carrying capacity of the bridge members, while DC and DW denote the dead load effects induced by structural components and the wearing surface, respectively. The live load effect and its equivalent dynamic effects are denoted by LL and IM, respectively, whereas the load factors are denoted by γ_{DC} , γ_{DW} and γ_{LL} . Moreover, the current load-carrying capacity C is described as:

$$\tag{2}$$

$$C = \varphi_c \varphi_s \varphi R_n$$

where φ_c , φ_s , φ and R_n are the condition factor, system factor, and the LRFD resistance factor, respectively, while R_n denotes the nominal resistance of bridge member. The load rating factor was calculated using the calibrated FEM, DF data, and the load value of the test vehicle utilised during the bridge testing, which its load was (52.7 (3) Ton). For Strength Limit I, we used values (1.25), (1.5) and (1.35) for factors γ_{DC} , γ_{DW} and γ_{LL} , respectively. As due to φ_c , φ_s , φ factors, value (1) was used for all them. Figure 15 shows the load rating factors (RF) of the test truck's passage in the second lane of all concrete and steel spans.

The load rating factor (RF) for girder No. 5, which is directly beneath the test vehicle, is (2.88) in the concrete span, as shown in the figure above. Additionally, RF for the girder No. 3 directly beneath the test vehicle in the steel span was (5.01). Generally, the load rating provides an estimation of the bridge carrying capacity with regard to the test truck load [16]. In this example, the results of the analysis suggest that the two girders G5 in span No.2 and G3 in span No.4 can respectively sustain 2.88 and 5.01 times the test truck load. More specifically, it can be said that girders G5 and G3 can support a truck weight of (146 tons) and (253.5 tons), respectively.

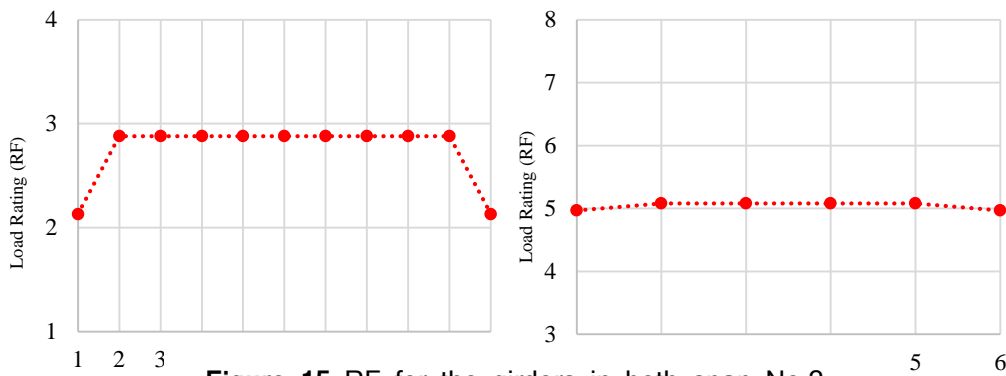


Figure 15 RF for the girders in both span No.2

(a) RF for concrete span

(a) RF for steel span (span

Modal Curvatures

The modal curvature of a bridge is used to evaluate whether or not the structure is damaged [26]. Reynders et al. [26] discovered that modal curvature determined by strain measurements is more accurate than modal curvature computed from displacement measurements. In our study, we used data from experimental and calibrated FEM to estimate the modal curvature. The following formula, Equation 4, is used to compute the curvature of the bridge girders:

$$k = \frac{\varepsilon_t - \varepsilon_b}{h} \quad (4)$$

Where ε_t and ε_b are the top and bottom strain of the girders; and h is the height of the bridge girder.

The girders under the load of the test truck were selected to estimate the modal curvature for all static, semi-static and dynamic tests cases. The selected girders were (G4, G5 and G6) for span No.2, while for span No.4 the chosen girders were (G1, G2 and G3). Figure 16 shows the modal curvature of the selected girders for tests cases. It is noted from the figure that the modal curvature of the steel span is smaller by about half. This is because of the bracing of the steel span, due to existing the distributed diaphragms [3]. The highest effect occurs at girder G4 at span No.2. The curvatures of the girder (G4) under cases (DC1) and (PC1) are almost the same and the highest. Similarly, the girder (G3) had the highest curvatures under cases (DC6) and (PC2). This indicates that both cases, semi-static cases and moving the truck with a speed of 10 Km/h, can be used to assess the curvature of bending members. Finally, curvatures modal performance of the bridge under the cases indicate that the modal curvature is found to be the same under different loading cases and the safety possibility of the bridge is high [26].

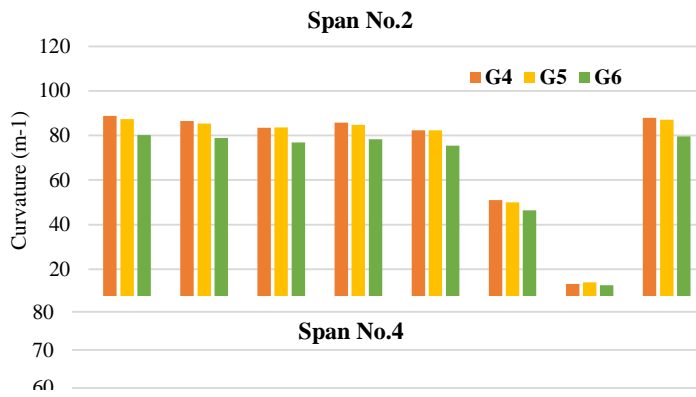


Figure 16 Girders Curvatures under different load

Neutral Axis Position

The neutral axis (NA) (DC1) and (PC1) as for stress distribution along PC1 were located at 0.8 m, respectively. Table 5 illustrates the NA of girders G4 and G5 under the cases, also shown the analytical NA that is calculated by the stresses of bottom of girder were obtained from FEM. From Table 5, the NA changes are in-between 0 – 15% from the analytical value. This reveals that no abnormal behaviour occurred [3].

er loading cases. The selected cases were (G3) at span No. 4. Figure 17 shows the of the concrete girder for cases DC1 and es DC6 and PC2 were at 1.38 m and 1.29 m, respectively. Figure 17 shows the of the concrete girder for cases DC1 and es DC6 and PC2 were at 1.38 m and 1.29 m, respectively. Figure 17 shows the of the concrete girder for cases DC1 and es DC6 and PC2 were at 1.38 m and 1.29 m, respectively.

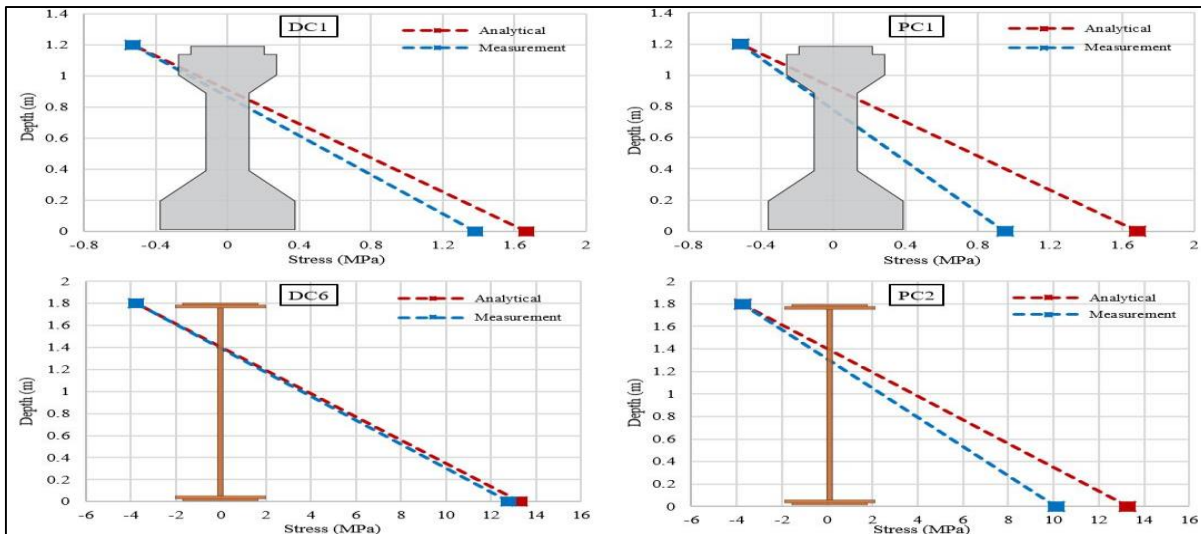


Figure 17 The neutral axis of the bridge girder

Table 5 Difference between actual NA and

Girder	G4		G3	
	DC1	PC1	DC6	PC2
Actual NA (m)	0.83	0.78	1.38	1.29
Analytical NA (m)	0.9	0.9	1.39	1.39
NA change %	8.5	15.3	0.7	7.75

Dynamic Behaviour Evaluation

To identify the modes of the shapes, the CSI Bridge software was used to perform a modal analysis on the calibrated finite element model. For both concrete and steel spans, modes were discovered. The first five modes of concrete and steel span are depicted in Figures 18 and 19, respectively.

The accelerations versus time histories obtained by six accelerometers deployed on the bridge were analysed to estimate the bridge's dynamic parameters from the experimental test. One of the other objectives of modal testing is to utilise the data to find any abnormal conditions that occur when the test vehicle is being moved. These dynamic findings may be followed over time to see whether there have been any significant changes

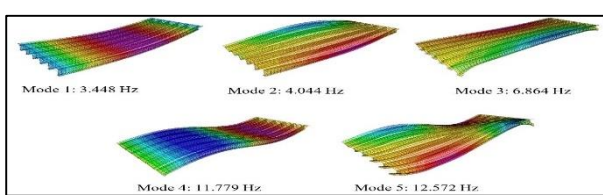


Figure 19The first five mode shanes of steel span

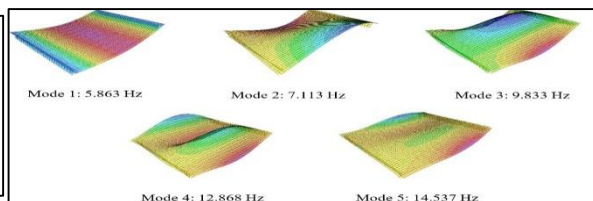


Figure 18The first five mode shapes of concrete span

The dynamic response was evaluated using acceleration measurements. It was found that the accelerations measurements in Z-direction at the ends of spans (ACC4Z and ACC6Z) are good for obtaining the dynamic response in the bridge. The highest accelerations of these accelerometers were utilized to set a relationship between the different speeds and the acceleration occurring in the bridge. Figure 20 shows a summary of the relation between the maximum acceleration under different speeds of the test truck for the two spans. The acceleration measurements under low-speed trucks contaminate by high noises that is because of the time of the truck that affected on the bridge span. In addition, the exponential equations (acceleration = 0.0584e^(0.0224×speed)) and (acceleration = 0.0191e^(0.0347×speed)) are a good fitting for the relation between maximum acceleration and truck speeds for Span No.2 and 4, respectively, and they can be used to detect the acceleration change of the bridge. The results show that the maximum accelerations (0.21g and 0.17g) are found to be lower than the standard value (0.26 g) [27].

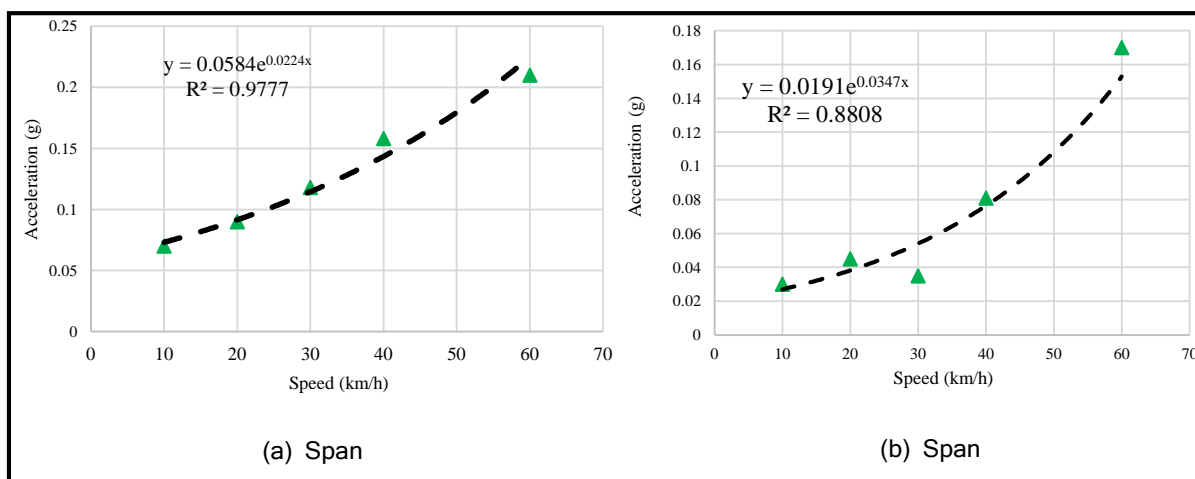
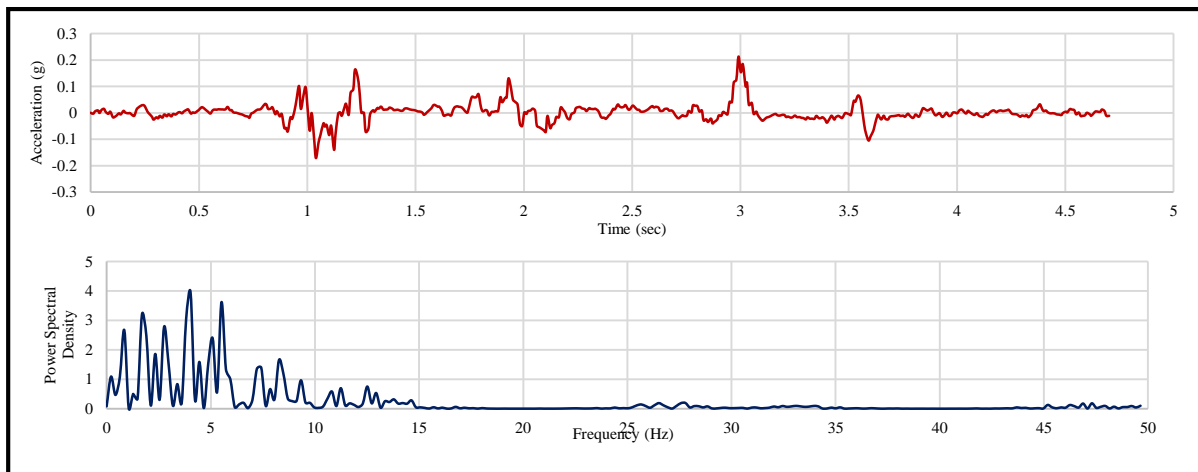


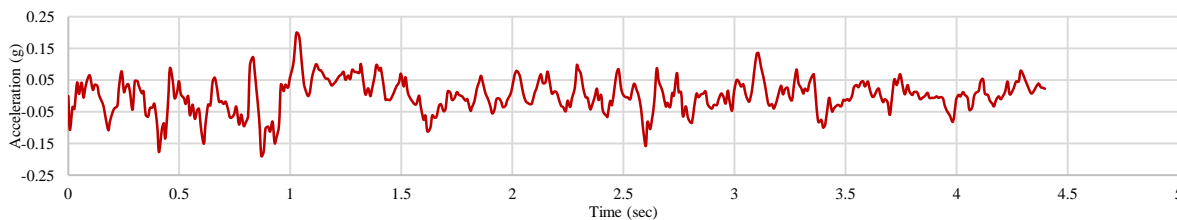
Figure 20Relationship between truck speeds and recorded

Here load cases DC5 and DC10 (test truck moved on Lane 2 with a speed of 60 km/h = 16.66 m/s) is considered for the dynamic analysis because it was discovered the maximum acceleration within these cases. It is seen based on the speed of the truck it takes

about 1.2 and 2.16 seconds to cross Span No.2 and No.4, respectively. Figure 21 shows the acceleration time histories of each measurement point and FFT analysis (Fast Fourier Transform) for load cases DC5 and DC10.



(a) Concrete Span



(b) Steel Span

Based on all the collected time histories, the operational modal analysis method is employed to identify the modal frequencies, damping ratio and mode shapes using (Artemis-Modal 6.0.2.0) software. The operational modal analysis, EFDD and SSI methods are generally used to identify modal parameters of linear systems using output-only measurements. Figures 22 and 23 present the estimated modal parameters, modes shapes and damping after modelled and processing the collected data from the experimental test using Artemis-Modal for both concrete and steel spans.

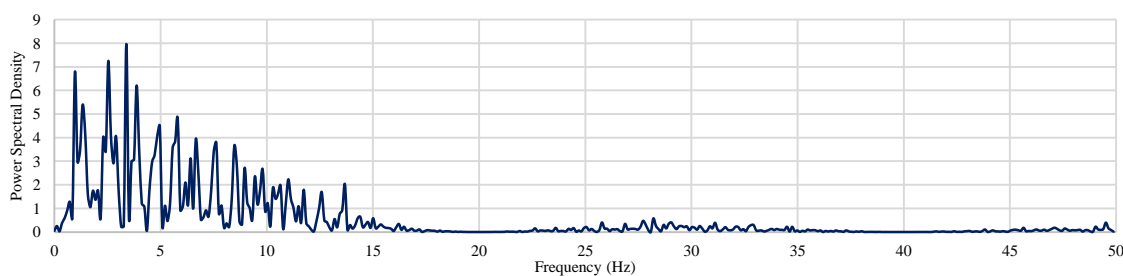
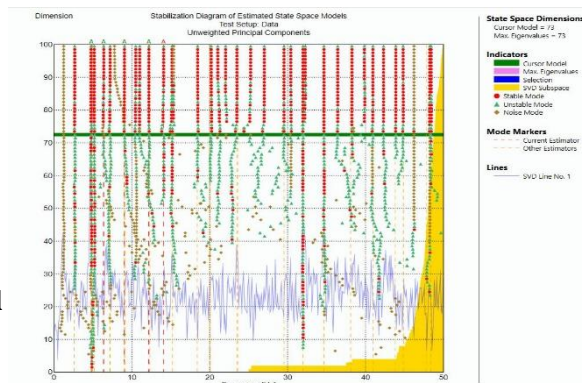
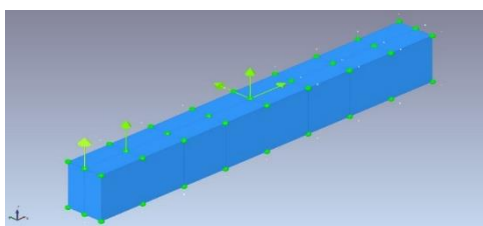


Figure 21 Readings and FFT analysis for DC5 and DC10 cases



Bridge girder modelling with accelerometers

Operational modal analysis

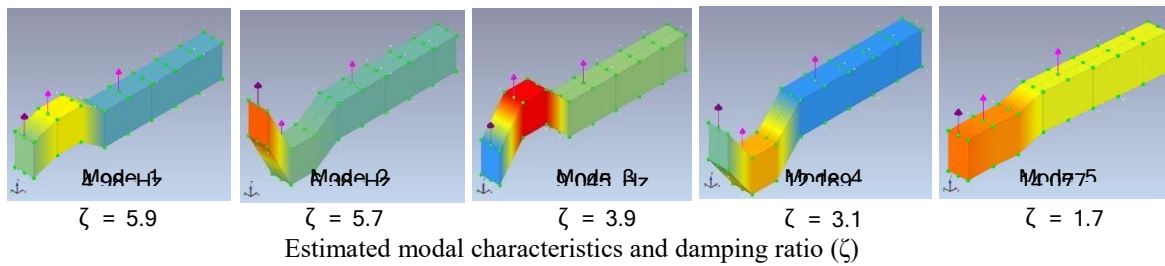
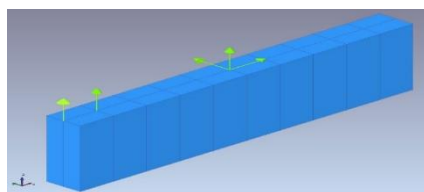
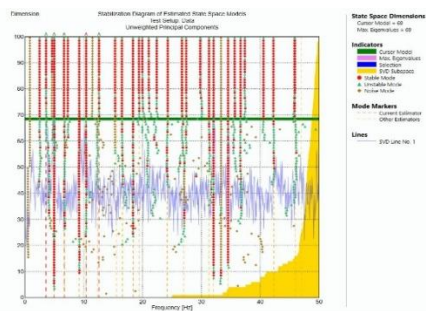


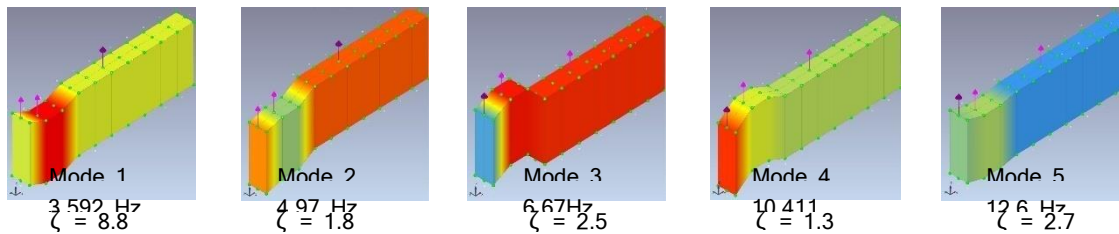
Figure 22 Operational Modal Analysis for concrete span



Bridge girder modelling with accelerometers



Operational modal analysis



Estimated modal characteristics and damping ratio (ζ)

Figure 23 Operational Modal Analysis for steel span

In addition, the dominant frequencies were identified. From the results of Artemis-Modal software, the dominant frequency is 4.98 and 4.97 Hz for the truck speeds 60 km/h along concrete and steel spans, respectively. Finally, the summary of frequency changes with truck speeds shows that the average dominant frequency is 4.975 Hz, whereas the design value is 2.35 Hz [27]. the calculated frequency ratios show that it is over than one, which means that the bridge behaviour is safe, and no abnormal conditions occurred, Table 6.

Table 6 Summary of Extracted Dominant Frequencies

Span	Concrete girders	Steel girders
Frequency (Hz)	4.98	4.97
Frequency Ratio %	2.12	2.11

The outcomes from the FE analysis of the bridge were also given in Table 7 to compare those from the experimental. Such data and dynamic response can be collected efficiently under operating traffic and can be evaluated to track any stiffness or boundary condition change.

Table 7 Comparison of modal frequencies

No.	Experimental (Hz)		FEM (Hz)		Difference (%)	
	Span 2	Span 4	Span 2	Span 4	Span 2	Span 4
Mode 1	4.98	3.592	5.86	3.44	17.67	4.23
Mode 2	6.38	4.97	7.11	4.04	11.44	18.71
Mode 3	9.045	6.67	9.83	6.86	8.67	2.84
Mode 4	12.189	10.411	12.86	11.77	5.5	13.05
Mode 5	14.077	12.6	14.53	12.57	3.21	0.23

Linearity Check

The linearity check of the bridge was carried out mainly to be able to calculate multiple presence factors by combining separate test results. Under regular operational loads, the bridge response should not reach ultimate response levels. As such, it would be possible to observe linear behaviour under given increasing load conditions. To check the linearity of the bridge, a random truck was chosen from the short-term monitoring data and given a name (LC), then compared with the test truck. After investigating, LC Truck was carrying a load of (832 KN) and has a speed of about (22 km/h). The displacement and strain data were picked from dynamic test cases with similar speed, which is (DC2 and DC7) to verify the linearity of concrete and steel spans as shown in Figures 24 and 25, respectively, and Table 8.

The weight increase ratio of the LC Truck to the test truck was found to be 1.57. It is also worth noting that the increased ratios of displacement and strain readings for the concrete span were by (1.77 and 1.32, respectively), but the increasing ratio for the steel span were (1.64 and 1.31, respectively). The linearity has been validated because the difference between the ratio increase in the readings of the LC truck and the ratio between the differences between the two weights was within the range of $15 \pm 1\%$ that was defined due to the change in axle number and total length of the truck as well as their location [23]. Finally, this provides proof that the bridge behaves linearly under operational loads until the load of 832 KN

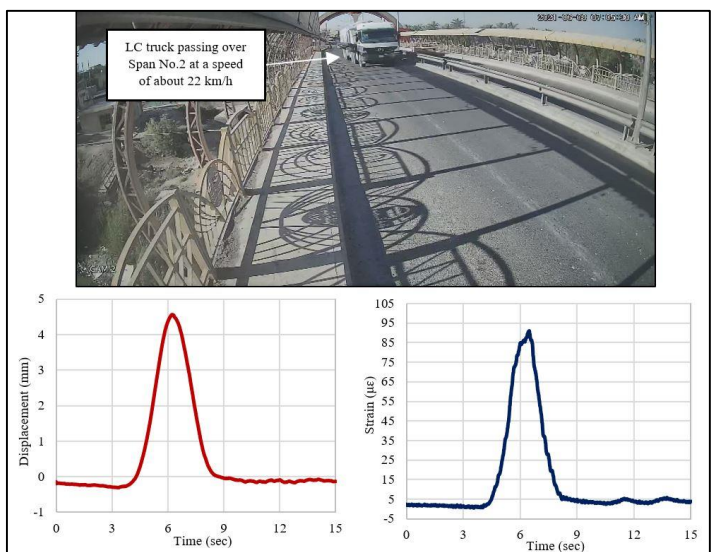


Figure 24 LC Truck data during passing the concrete span

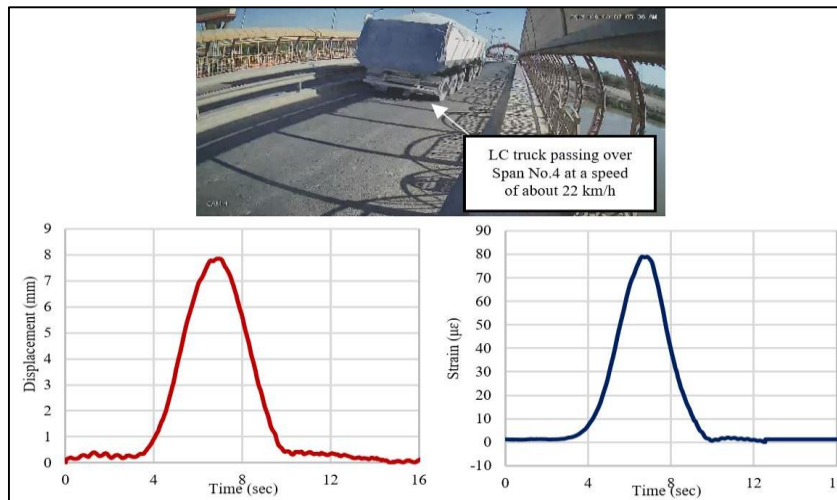


Figure 25LC Truck data during passing the steel span

Table 8Linearity Ratio between LC truck and test truck

Case name	Truck	Total weight (KN)	Displacement (mm)		Strain ($\mu\epsilon$)	
			Span No. 2	Span No. 4	Span No. 2	Span No. 4
DC2 and DC7	Test truck	527	2.53	4.75	68.31	60.61
LC	LC truck	832	4.48	7.82	90.1	79.8
Ratio		1.57	1.77	1.64	1.32	1.31

Maximum Stresses Check

The maximum sectional stress distributions are evaluated depending on passing the same long truck that resulted maximum displacements with allowable stresses of the steel grade and concrete. An analysis of the long truck moving over the bridge was performed using the calibrated FEM. Figure 26 illustrates the stress performance of the bridge (girder 5 within Span No.2 and girder 3 within Span No.4) under the long truck.

The positive and negative stresses refer to compression and tension stresses of structures members. From Figure 26, the maximum tension stress (19.01 MPa) was observed at mid-span of steel girder (girder 3). In addition, the maximum tension stress (2.15 MPa) was obtained at mid-span of girder 5. The maximum, minimum and overall bending and shear stresses reveal that the bridge is safe under the abnormal load case, where the observed stresses are lower than the allowable stresses of steel grade ST52-3 and the concrete of girder

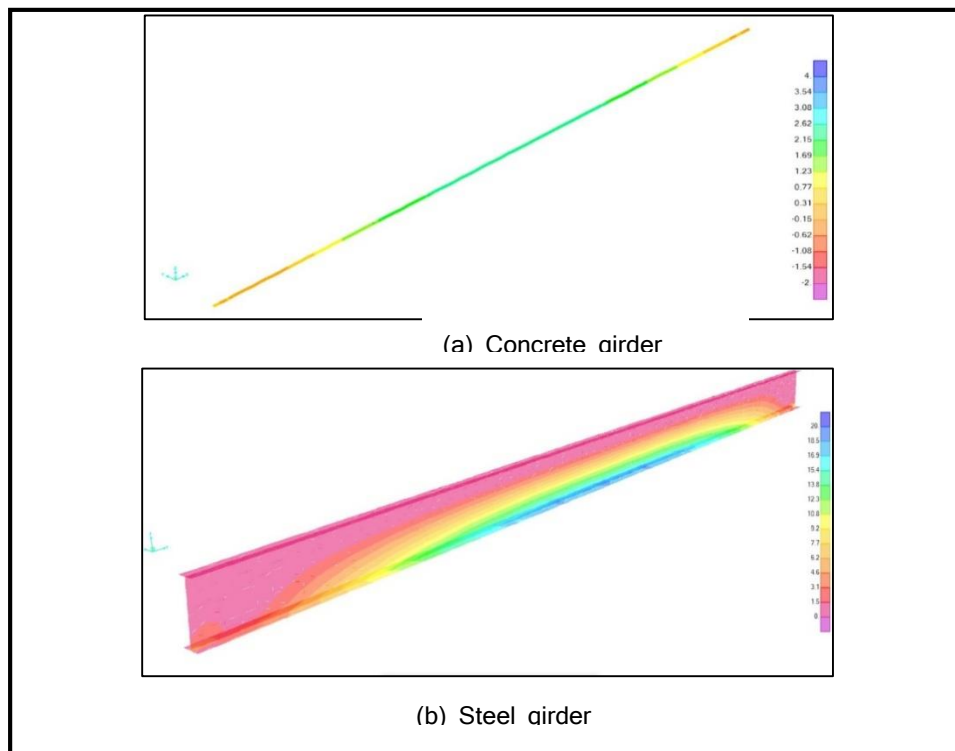


Figure 26 Distribution of stresses in the concrete and steel girder

Conclusion

The following is a summary of some of the particular results for this bridge:

- Static and dynamic testing results were acquired through the experimental data. These results were employed for improving the updated FEM of the bridge. The DF and RF results from the updated FEM were obtained to be in good agreement and reliable. Hence, the calibrated FEM can be adopted reliably for advanced analysis of the bridge.
- When compared to experimental and FEM methods, the DF of live load computed by AASHTO standards gives more conservative findings. The static load case's DF is 0.2, which is smaller than the AASHTO code's 0.60. The updated FEM value of 0.2 for this parameter.
- Maximum deflections in static and dynamic scenarios are well below the $(L/800)$ limit, and deflections are significantly lower than the AASHTO code-based $L/800$.
- The load rating factor has been determined with the requirements of AASHTO and experiment results. Rating factors of Strength Limit I were 2.88 for concrete span and 5.01 for steel span both for test truck for a single lane. As a result, it was possible to determine the load-carrying capacity for the bridge.
- In addition, the curvature modal, neutral axis and dynamic characteristics are estimated to assess the bridge girders performance under static and dynamic loads.
- For the bridge assessment, the results show that the bridge behaviour is safe in different indices, such as maximum displacement, modal curvature, neutral axis, and frequency changes. All these indices are reported to be lower than the standard values of AASHTO. Furthermore, the evaluation of the measurement shows that no abnormal condition occurred.
- The study found that bridge condition assessments could be completed quickly and accurately without stopping traffic or disrupting bridge operations. As a result, the methodology presented in the study may be used to bridge in the same population.
- Based on the findings, it is shown that the bridge has sufficient load carrying capacity and the bridge can carry large truck loads. For the behaviour under heavy truck loading, the 832 KN truck was employed from short-term monitoring to check linearity,

displacement and stresses to obtain the bridge capacity and safety for the most critical condition. As a result, the bridge can continue to serve and no-load posting is necessary based on the results given in this study.

REFERENCES

1. AASHTO LRFD bridge design specifications. 2008: Fourth edition with 2008 interim revisions. Washington, D.C. : American Association of State Highway and Transportation Officials, [2008] ©2007.
2. Liu, Z., K. Freeseaman, and B.M. Phares, Evaluation of the need for negative moment reinforcing in prestressed concrete bridges in the view of service loads. *Engineering Structures*, 2020. 207: p. 110206.
3. Kaloop, M.R., et al., Service-Life Evaluation of Existing Bridges Subjected to Static and Moving Trucks Using Structural Health Monitoring System: Case Study. *KSCE Journal of Civil Engineering*, 2020. 24(5): p. 1593-1606.
4. Algohi, B., B. Bakht, and A. Mufti, Long-term study on bearing restraint of a girder bridge. *Journal of Civil Structural Health Monitoring*, 2017. 7(1): p. 45-55.
5. El-Sisi, A.E.-D.A., et al., Field-testing and numerical simulation of vantage steel bridge. *Journal of Civil Structural Health Monitoring*, 2020. 10(3): p. 443-456.
6. Nick, H., et al., Damage identification in steel girder bridges using modal strain energy-based damage index method and artificial neural network. *Engineering Failure Analysis*, 2021. 119: p. 105010.
7. Nguyen, D.H., et al., Damage detection in girder bridges using modal curvatures gapped smoothing method and Convolutional Neural Network: Application to Bo Nghi bridge. *Theoretical and Applied Fracture Mechanics*, 2020. 109: p. 102728.
8. Jahan, S., et al., A Fuzzy Krill Herd Approach for Structural Health Monitoring of Bridges using Operational Modal Analysis. *Iranian Journal of Science and Technology, Transactions of Civil Engineering*, 2021. 45(2): p. 1139-1157.
9. Kalyankar, R. and N. Uddin, Axle detection on prestressed concrete bridge using bridge weigh-in-motion system. *Journal of Civil Structural Health Monitoring*, 2017. 7(2): p. 191-205.
10. Faraz, S., et al., Sources of errors in fatigue assessment of steel bridges using BWIM. *Journal of Civil Structural Health Monitoring*, 2017. 7(3): p. 291-302.
11. Algohi, B., A. Mufti, and D. Thomson, Detection of speed and axle configuration of moving vehicles using acoustic emission. *Journal of Civil Structural Health Monitoring*, 2018. 8(3): p. 353-362.
12. Lydon, M., et al., Improved axle detection for bridge weigh-in-motion systems using fiber optic sensors. *Journal of Civil Structural Health Monitoring*, 2017. 7(3): p. 325-332.
13. Dong, C.-Z., S. Bas, and F.N. Catbas, A portable monitoring approach using cameras and computer vision for bridge load rating in smart cities. *Journal of Civil Structural Health Monitoring*, 2020. 10(5): p. 1001-1021.
14. Xiao, P., et al., Development of video analytics with template matching methods for using camera as sensor and application to highway bridge structural health monitoring. *Journal of Civil Structural Health Monitoring*, 2020. 10(3): p. 405-424.
15. Jeon, J.-C. and H.-H. Lee, Development of displacement estimation method of girder bridges using measured strain signal induced by vehicular loads. *Engineering Structures*, 2019. 186: p. 203-215.
16. Sun, Z., D.M. Siringoringo, and Y. Fujino, Load-carrying capacity evaluation of girder bridge using moving vehicle. *Engineering Structures*, 2021. 229: p. 111645.
17. Friswell, M. and J.E. Mottershead, *Finite element model updating in structural dynamics*. Vol. 38. 2013: Springer Science & Business Media.
18. CSI BRIDGE, *Integrated 3-D bridge analysis, design and rating*. V.22: CSI Analysis Reference Manual.
19. Manual, C.A.R., *sap2000 Integrated solution for structural analysis and design*. V. 21.
20. Instruments, N., *LabVIEW User Manual*. 2003 Edition.
21. Olaszek, P., M. Łagoda, and J.R. Casas, Diagnostic load testing and assessment of existing bridges: examples of application. *Structure and Infrastructure Engineering*, 2014. 10(6): p. 834-842.
22. Casas, J., A. Znidaric, and P. Olaszek, *Recommendation on the use of soft, diagnostic and proof load testing*. Deliverable D16. EU project ARCHES. Brussels. 2009.
23. Dong, C., et al., Bridge load testing for identifying live load distribution, load rating, serviceability and dynamic response. *Frontiers in Built Environment*, 2020. 6: p. 46.
24. Smolenski, P.J., *Field instrumentation and live load testing to evaluate behaviors of three reinforced concrete bridge decks*. 2004, Montana State University-Bozeman, College of Engineering.
25. Bridges, T.O.S.o., *The manual for bridge evaluation*. 2011: AASHTO.
26. Reynders, E., et al., Damage identification on the Tilff Bridge by vibration monitoring using optical fiber strain sensors. *Journal of engineering mechanics*, 2007. 133(2): p. 185-193.
27. Gaunt, J.T. and C.D. Sutton, *Highway bridge vibration studies*. 1981.
28. Roensch, S., "Finite Element Analysis". Roensch & Associates, 2008.

29. Bień, J., M. Kuźawa, and T. Kamiński, Strategies and tools for the monitoring of concrete bridges. *Structural Concrete*, 2020. 21(4): p. 1227-1239.
30. Chen, H.-P., *Structural health monitoring of large civil engineering structures*. 2018.